TECHNISCHE MECHANIK
an open access journal

journal homepage: www.ovgu.de/techmech

Tech. Mech., Vol. 40, Is. 1, (2020), 59–65

Received: 02.09.2019
Accepted: 20.01.2020
Available online: 20.02.2020

Development of a thermomechanically coupled damage approach for modeling woven ceramic matrix composites

Marie-Christine Reuvers[1]*, Shahed Rezaei[1], Tim Brepols[1] and Stefanie Reese[1]

[1] RWTH Aachen University, Institute of Applied Mechanics, Mies-van-der-Rohe-Str. 1, 52074 Aachen, Germany

Abstract: Ceramic matrix composites (CMCs) as an enhancement of classical technical ceramics overcome limitations such as low fracture toughness and brittle failure under mechanical or thermomechanical loading. Their low weight and high temperature stability makes them attractive for use in various fields, especially aerospace industry, where they improve engine efficiency as substitutions for metal components. Despite their positive attributes current CMCs lack well established material property design databases for a reliable use in critical aerospace structures. Demonstrating the durability and lifespan of this relatively new class of materials is the present task. Therefore their failure mechanisms need to be investigated further, taking into account the extensive range of temperatures the components are subjected to. This contribution deals with the successive development of a woven representative volume element (RVE) for arbitrary CMCs. In contrast to previously developed approaches, the introduced model combines various damage formulations. The fiber bridging effect is governed using a cohesive zone (CZ) formulation to adress the debonding mechanism in the weak interface between matrix and reinforcement and a continuum mechanical approach to account for matrix damage. To cover the temperature dependency of the material parameters, thermal coupling is included in both element formulations.

Keywords: CMC, RVE, cohesive zone,continuum damage, composites, woven

1 Introduction

Materials in aerospace engines are exposed to high temperatures, oxidizing environments and have to withstand numerous load cycles during their lifetime. Until now most of the engines components are made out of metal alloys which have a rather short lifespan. Current research therefore focuses on the development of a new class of materials to replace these metal components with ceramics to increase temperature resistace and lifetime under high cyclic loading while reducing weight at the same time. Ceramics are inorganic materials with a high service temperature and elastic modulus. They are designed to be corrosion resistant and lightweight, however ceramics have a very low crack resistance and are therefore considered brittle materials see Krenkel (2008), Chawla (2013). To increase fracture thoughness classic ceramic matrices are improved with a reinforcement. Ceramic matrix composites (CMCs) make up a rather new class of engineered ceramic materials, consisting of matrix and fiber reinforcement. The fibers, produced as fiber bundles or so called toes, are often manufactured as a woven mesh to form 2D or 3D composites. Characteristically CMC components often consist of the same or similar materials for example silicon carbide(SiC/SiC) or aluminium oxide (Ox/Ox). Depending on the presence of oxygen, CMCs are categorized into non-oxide (NO-CMC) or oxide (O-CMC) materials. NO-CMCs have a higher temperature resistance, whereas O-CMCs are more corrosion resistant. To compensate for the low corrosion resistance, fibers of non-oxide ceramics are coated with boron nitride (BN), forming an interphase between fiber and matrix Bansal (2006). In order to increase the fracture toughness of the ceramic with the reinforced fibers, the interface between the two compounds is the deciding factor. A weak interface is desirable to achieve a separation between matrix and fiber in the case of damage. During failure, cracks will first form in the ceramic matrix of the composites and propagate through the material. Once a fiber-matrix interface is reached, the crack will deflect there, starting a separation process between the two components. Undamaged fibers remain, briding the open crack. In the case of ultimate failure, the fibers start to slide along the matrix adding an additional fracture mechanism to the otherwise brittle material which results in a pseudo-plastic material response Evans and Zok (1994). If the fibers are coated, the interphase works as a protective layer. With a material fracture energy lower than the interface resistance between fiber and coating, the crack is supposed to deflect in the interphase, leaving a thin film of coating to the fibers to ensure corrosion resistance Bansal and Lamon (2014). Due to production processes to the authors best knowledge to this day it is not possible to produce a strong fiber-coating interface with BN, therefore a crack will lead to debonding between fiber and coating Rebillat et al. (2000a). Under temperature the maximum strength of CMCs decreases due to material degradation, resulting in a lower Young's modulus and a softened material response Bansal (2006). In addition the location of the deflecting crack in coated CMCs is shown to shift to the matrix-coating interface, due to changes in the BN maximum strength Trice and Halloran (1999), Guo and Kagawa (2001).
On the numerical side brittle fracture has been modeled by many authors using cohesive elements. For example Samimi et al. (2009, 2011) has developed a CZ formulation to acount for delamination in brittle interfaces, using an effective separation law. Rezaei et al. (2017) extended the formulation to predict fracture in micro/nano coating systems between grain boundaries and also simulated plastic behavior between multiple grains by using molecular dynamics (MD) simulations to calculate the

* E-mail address: marie.reuvers@ifam.rwth-aachen.de
doi: 10.24352/UB.OVGU-2020-014

traction-separation-law (t-s-law) Rezaei et al. (2019). The inclusion of fiber briding has been investigated for example by Höwer et al. (2018) in the case of delaminating sandwich panels. To compare expermimental results for SiC/SiC material to numerical simulations Kumar and Welsh (2012); Kumar (2013) investigated the failure mechanisms between but also within plies and extended the CZ formulation to include fiber bridging for more accurate results Kumar (2017); Kumar et al. (2018). Mital et al. (2009) studied different methods to efficiently determine the elastic properties of melt-infiltrated (MI) SiC/SiC composites using multiscale laminate analysis, finite element analysis etc..Chaboche and Maire (2002) developed a micromechanics bases continuum damage model including second order tensor while Marcin et al. (2011) adressed the woven characteristics of CMCs with a macroscopic damage model using inetrnal variables. A general overview of modeling schemes for the damage mechanisms of CMCs at multiple scales, can be found in Baranger (2017). Experimental data for different SiC/SiC composites and scales under room and elevated temperatures can be found for example in Rebillat et al. (2000b), Guo and Kagawa (2001), Hinoki et al. (2003) and Morscher (2010). The influence of thermal loading on interface fracture has also been studied by various authors. E.g.Dandekar and Shin (2011) included a temperature dependence in the traction-separation-law, acounting for a softer interface response under temperature using MD simulations to parametrize the t-s-law. To investigate the evolving heat transfer through interfaces Hattiangadi and Siegmund (2004) introduced a temperature jump in the cohesive formulation modeling fiber bridging under bending and buckling deformation. Özdemir et al. (2010) also included fiber briding as well as a damage dependend heat flux to simulate crack closure and Wu and Wriggers (2015) took up the idea to model the influence of the transition zone between cement paste and aggregates on the thermal properties of concrete. Quasi brittle crack propagation in a thermo-hyperelastic material including heat generation within the cohesive zone due to the fracture process is simulated by Fagerström and Larsson (2008) including a discontinous heat flux across the interface. Focussing on the time evolution of displacement and temperature fields before debonding Paggi and Sapora (2013), Sapora and Paggi (2014) established a coupled model formulation in analogy to contact mechanics between rough surfaces for photovoltaics.
In this work a material model combining various damage formulations based on Rezaei et al. (2017) and Brepols et al. (2017) is established, to model the characteristic failure mechanisms in CMC. Unlike existing modeling approaches for CMC failure behavior in this formulation a cohesive zone model is combinded with a gradient extended continuum damage model to take various damage mechanisms of CMC (e.g. matrix cracking, interface debonding) into account. The model is then extended to include thermal phenomena, as for example the decrease of interface resistance under thermal loading as well as the heat flux across the interface and then tested in different numerical examples.

2 Modeling Approach

2.1 Cohesive Zone

Mechanical Problem Separation at the fiber-matrix interface is modeled using a cohesive zone formulation based on the work of Geubelle and Baylor (1998), Ortiz and Pandolfi (1999) and Rezaei et al. (2017) with a bilinear traction-separation-law. Two bodies B_t^+ and B_t^- are considered in 2D which are connected by a cohesive region see Fig.1. The Helmholtz free mechanical energy is defined as

$$\psi_{cz}(g_s, g_n) = \frac{1}{2}(1-d)k_0\lambda^2 + \frac{1}{2}k_p\langle -g_n\rangle^2, \tag{1}$$

where $\lambda = \sqrt{\langle g_n\rangle^2 + \beta^2 g_s^2}$ describes the effective separation of the cohesive zone, which depends on the gap in normal g_n and shear g_s direction. The amount of shear contribution is controlled via the parameter β to consider materials with anisotropic damage behavior. the influence on the traction can be seen in Fig.1. Further material parameters are k_0 which can be interpreted as the undamaged stiffness of the cohesive zone. To prevent penetration of the two bodies, if the normal gap becomes negativ ($g_n < 0$), a penalty term is introduced, depending on the penalty parameter k_p. Analogously to the gap the traction vector $\boldsymbol{t}$ is decomposed into a normal t_n and a shear traction t_s and follows to

$$\boldsymbol{t} = \left\{ \begin{array}{rcl} t_n & = & \partial_{g_n}\psi_{cz} \\ t_s & = & \partial_{g_s}\psi_{cz} \end{array} \right. \begin{array}{l} = (1-d)k_0\langle g_n\rangle - k_p\langle -g_n\rangle \\ = (1-d)k_0 g_s\beta^2. \end{array} \tag{2}$$

Similarly an effective traction t can be defined as

$$t = \partial_\lambda\psi_{cz} = \sqrt{t_n^2 + \beta^{-2}t_s^2} = (1-d)k_0\lambda. \tag{3}$$

The damage parameter d is chosen to follow the softening-behavior of the bilinear traction-separation law see Fig.2 and follows to

$$d = \left\{ \begin{array}{ll} 0 & \text{if } \lambda < \lambda_0 \\ \dfrac{\lambda_f}{\lambda_f - \lambda_0}\dfrac{\lambda - \lambda_0}{\lambda} & \text{if } \lambda_0 < \lambda < \lambda_f \\ 1 & \text{if } \lambda_f < \lambda. \end{array} \right. \tag{4}$$

If the maximum strength t_0 is reached at the corresponding amount of separation (λ_0), the cohesive zone starts to fail. The damage now develops nonlinearly until the maximum elongation λ_f is reached. Via Integration of the traction-separation-law the fracture energy

$$G_c = 0.5 t_0 \lambda_f \tag{5}$$

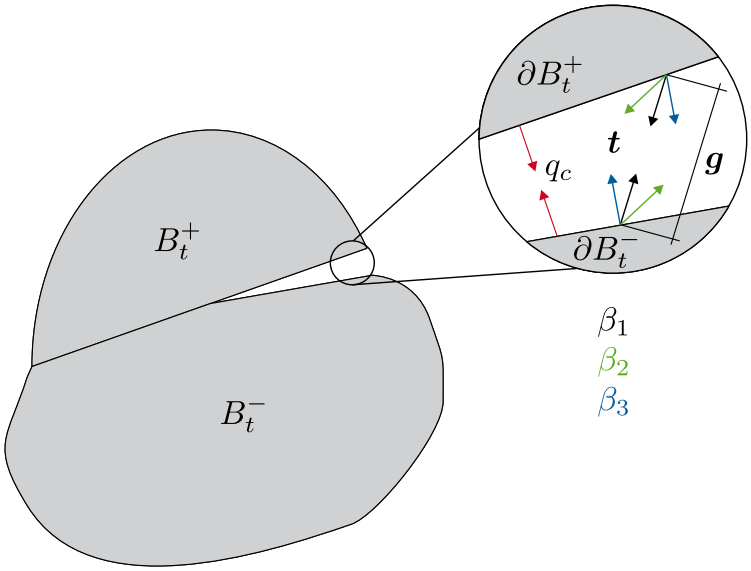

Fig. 1: Separation of two bodies. Gap and traction vectors for different parameters β.

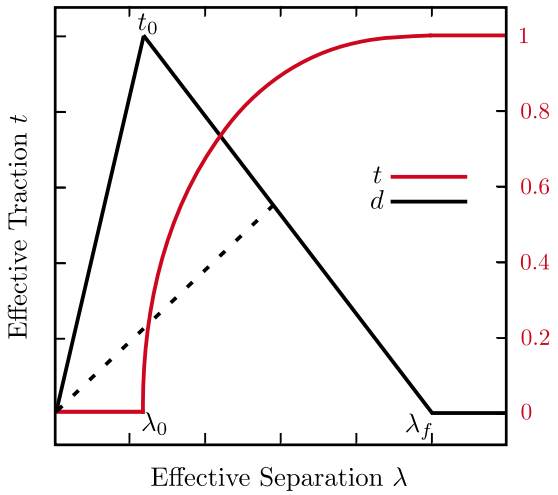

Fig. 2: Effective traction t over effective separation λ and damage evolution.

can be determinded, which serves as an important material parameter for the characterization of the overall interface resistance.

Thermal Problem Ideally there is no temperature jump and no thermal flux jump when two bodies of different materials are assumed to be bonded perfectly. However in reality a perfectly bonded interface doesn't exist, due to either pre-existing microcracks or imperfections as for example pores at the interface or the debonding induced by external loads. Therefore in this application a lowly-conducting interface is assumed, allowing for a jump of the temperature based on the Kapitza assumption (Sapora and Paggi (2014)).
In anaolgy to the work of Özdemir et al. (2010) and Wu and Wriggers (2015) a temperature jump g_θ in normal direction is introduced to the gap (see Fig. 1). Taking into account only stationary problems a heat flux

$$q_c = -((1 - d_c^\theta)k_s + k_a)g_\theta \tag{6}$$

is introduced through Fourier's law, depending on the heat conductivity of the solid phase k_s and the heat conductivity of air k_a. d_c^θ is a thermal damage variable for illustrating the progressive thermal resistance due to interface cracking

$$d_c^\theta = \begin{cases} \dfrac{\lambda}{\lambda_f} & \text{if } \lambda < \lambda_f \\ 1 & \text{if } \lambda_f < \lambda. \end{cases} \tag{7}$$

It starts to develop linearly even before the formation of the main interface crack to take into account the effect of microcracks forming in the elastic regime of the cohesive zone. Due to limited available data on the thermal behavior of the closing surfaces, the thermal model in this research stage does not consider crack closure. In addition to conduction, temperature has also been shown to have an influence on the material parameters of CMCs interfaces (see Trice and Halloran (1999) and Guo and Kagawa (2001)). To capture the softening behavior of the interface restistance in CMCs under temperature loading the Helmholtz free mechanical energy of the cohesive zone is extended with a temperature softening term

$$\psi_{cz}(g_s, g_n, \theta_m) = \frac{1}{2}(1 - d)k_0(1 - c_c\theta_m)\lambda^2 + \frac{1}{2}k_p\langle -g_n\rangle^2, \tag{8}$$

depending on a temperature softening parameter c_c which has to be determined experimentally, as well as the mid-temperature of the cohesive zone θ_m. The effective traction then follows to

$$t = \partial_\lambda\psi_{cz} = (1 - d)k_0(1 - c_c\theta_m)\lambda. \tag{9}$$

Thermal effects like heat radiation and convection are neglected at this stage of the model development and the model formulation is only valid for service temperatures.

2.2 Bulk Material

To model damage in the matrix material, an elastic gradient-extended damage formulation based on a more general model by Brepols et al. (2017, 2018) is used. The formulation of Brepols et al. (2017, 2018) also takes plasticity into account which is neglected in this work due to the brittle material behavior. The free energy

$$\psi = (1 - D)^2\psi_e(\boldsymbol{\varepsilon}_e) + \psi_d(\xi_d) + \psi_{\bar{d}}(D - \bar{D}, \nabla\bar{D}) \tag{10}$$

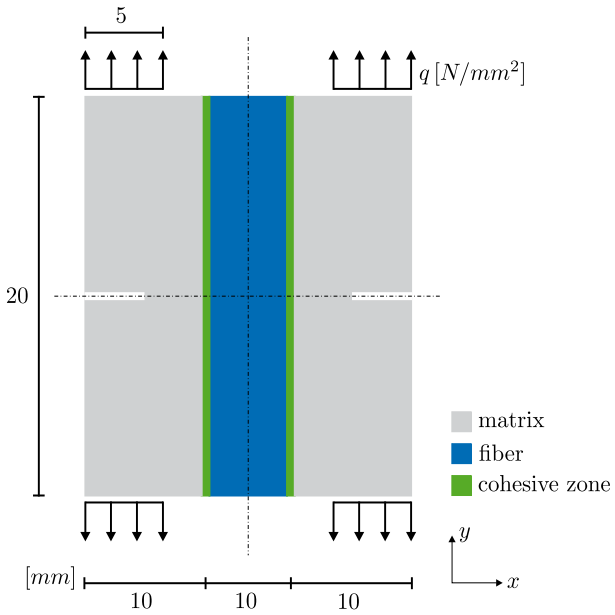

Fig. 3: Mechanical model

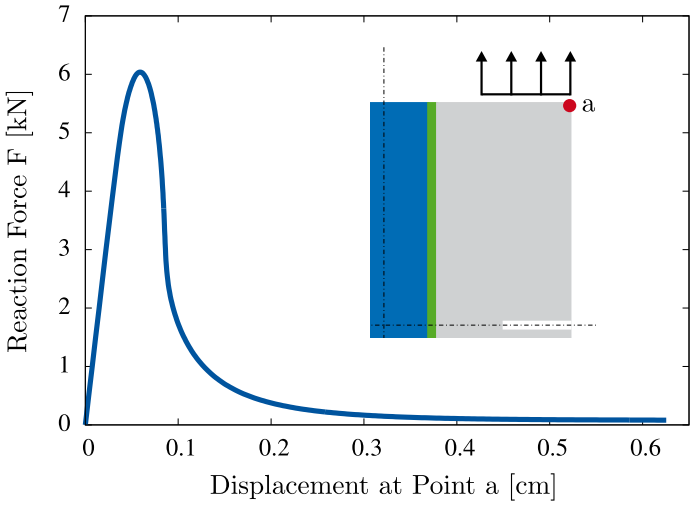

Fig. 4: Force-displacement curve in load-direction

is decomposed into three parts, the first being the elastic energy $\psi_e = \frac{1}{2}\boldsymbol{\varepsilon}_e \cdot \mathbb{C}[\boldsymbol{\varepsilon}_e]$. A damage hardening term $\psi_d = r\left(\xi_d + \frac{\exp(-s\xi_d)-1}{s}\right)$, depending on the damage material parameters r and s is introduced as well as a micromorphic extension $\psi_{\bar{d}} = \frac{A}{2}\nabla\bar{D}\cdot\nabla\bar{D} + \frac{H}{2}(D-\bar{D})^2$, depending on the micromorphic damage $\bar{D}$, its first gradient and the penalty parameter H as well as the parameter A, that implicitly introduces an 'internal material length', to achieve mesh independent results (see Forest (2009)). For a detailed model description the reader is referred to Brepols et al. (2017, 2018).

3 Numerical Examples

3.1 Crack deflection at the interface

A pre-cracked matrix (length of the notch = 2.5mm), reinforced with a single fiber on microlevel is modeled in the finite element program FEAP, using hexahedral cohesive zone elements with linear shape functions at the interface (see Fig. 3). Due to its minimal thickness, the coating is neglected during simulation, its effect is however modeled in the cohesive zone. In order to proof that the fiber is being spared during the interface separation process, both fiber and matrix are simulated as bulk material. In Table 1 and 2 the arbitrarily chosen material parameters for the presented example are displayed seperately for the two element formulations, with Λ and μ being the Lamé constants and Y_0 the onset of damage. Throughout the plane strain simulation the load is controlled by means of the arclength method, only one half of the structure (4880 elements) is plotted (due to symmetry).

Tab. 1: Cohesive zone material parameters

$\lambda_0\,[\mu m]$	t_0 [MPa]	$\beta[-]$	$\lambda_f\,[\mu m]$	$k_p[-]$
0.5	1.0	0.5	10	100

Tab. 2: Matrix and fiber material parameters

Λ [MPa]	μ [MPa]	Y_0 [MPa]	A [MPamm^2]	H [MPa]	r [−]	s [MPa]
5000	7500	0.1	10	10^5	0.5	0.1

During the simulation it can be seen in reaction force-displacement-curve (see Fig. 4) and the damage plots (see Fig. 5), that the crack evolves at the notch of the pre-crack where the stress concentrates. The crack then propagates along the matrix until it reaches the interface. As soon as the maximum traction of the cohesive elements at the interface is exeeded, the crack deflects now gradually separating the two components, fiber and matrix from each other. It can be demonstrated, that the fiber remains undamaged during the whole simulation. Since the material parameters are arbitrarily chosen, the resulting reaction force-displacement curve in Fig. 4 does not reflect the actual brittle material behavior. However the intention of the example in modeling crack deflection at the interface by the combination of different damage models is fullfilled.

3.2 Interface resistance under temperature

As a second example the interface resistance under temperature influence is simulated in the finite element program FEAP via a double cantilever beam (DCB). On the mesoscale the two bulk materials, modeled using standard thermomechanically coupled,

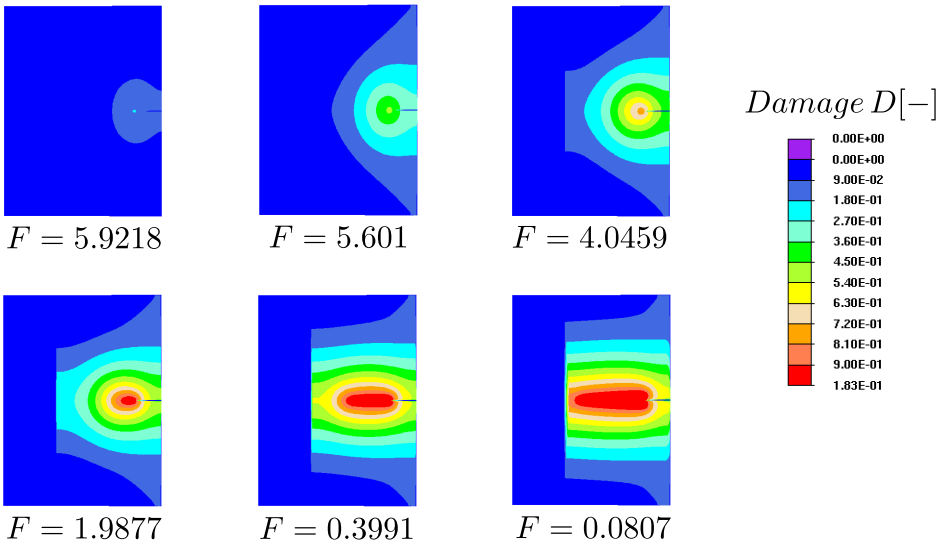

Fig. 5: Damage evolution at the notch

linear elastic FEAP elements, represent CMC plies, each consisting of matrix, coating and reinforcement. The interface between those plies is modeled using a layer of cohesive elements. The dimensions as well as the boundary conditions for the problem can be found in Fig. 6 and Table 3 and 4. At the beginning of the plane strain simulation the body is heated up to a constant temperature between $0°C$ and $500°C$. Then holding the temperature constant, the displacement is applied linearly over time, separating the two plies.

The reaction force at the loading point over the corresponding displacement is displayed in Fig. 7. One can observe a decrease in the maximum force with increasing temperature, which can be explained in accordance to Dandekar and Shin (2011) by an overall reduced interface resistance between the plies. In addition at higher temperatures the failure starts earlier due to the degradation of the interface characteristics.

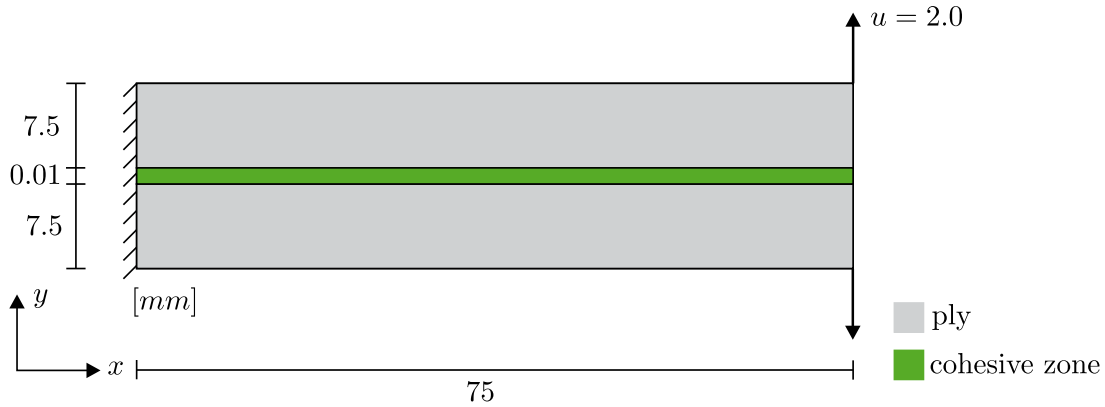

Fig. 6: Double Cantilever beam under thermal and mechanical loading.

Tab. 3: Thermal cohesive zone parameters

λ_0 [μm]	t_0 [MPa]	β[−]	λ_f [μm]	k_p[−]	k_c [W/mK]	k_a [W/mK]	c_c [1/K]
0.5	1.0	0.5	10	100	9.8	0.0262	0.001

Tab. 4: Thermal bulk material parameters

E [MPa]	ν [−]	α_T [1/K]	k [W/mK]	c [J/kgK]
380	0.2	0	9.8	0

4 Conclusion and outlook

A new strategy for modeling the different damage mechanisms in ceramic matrix composites is presented and tested at different material levels. With the combination of cohesive elements for brittle interface fracture and a continuum damage formulation for elastic materials it can be shown that the model is able to capture both, matrix cracking as well as the characteristic crack deflection at the fiber/matrix interface. The model formulation is then extended to include thermal effects, showing a decrease in interface resistance under elevated temperatures. In addition the effect of an earlier damage initiation due to material degradation is captured nicely in the simulation.

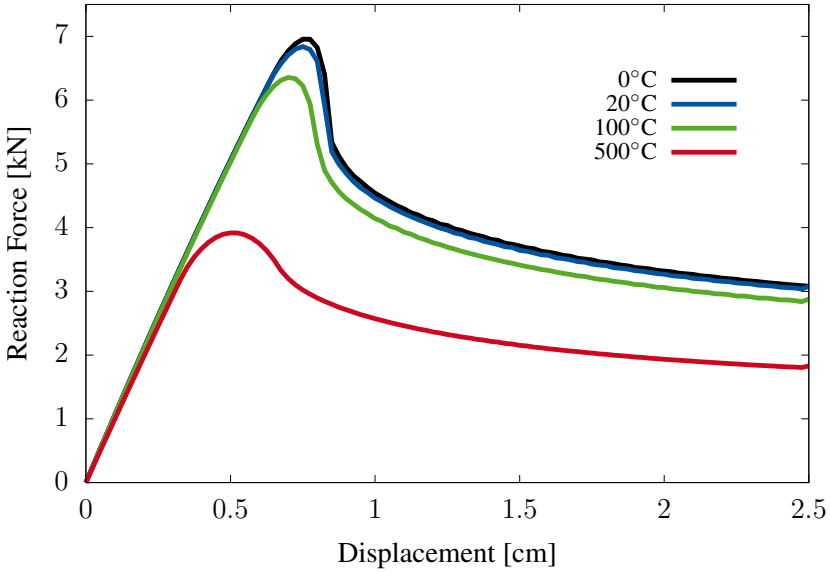

Fig. 7: Force-displacement curve of DCB under constant temperatures.

As the cohesive zone formulation in this work only includes a temperature dependence of the material stiffness, for future applications other material parameters who are shown to change significantly under temperature (e.g. thermal conductivity of solid or gaseous phase) will be thermocoupled. Furthermore the interface model at this point does not contain fiber briding in mechanical or thermal form. The formulation will be extendend thereby, introducing an additional heat flux in tangential direction to account for fibers with arbitrary directions and also the continuum damage model will be extended to include thermal effects. In addition there is a need to determine accurate material parameters for the interface to compare the simulation results to realistic experimental data. To simulate the real material behavior the formulation will then be extended to 3D to model woven material structures, characteristically for CMCs.

References

N. P. Bansal. *Handbook of ceramic composites*, volume 200. Springer Science & Business Media, 2006.

N. P. Bansal and J. Lamon. *Ceramic matrix composites: materials, modeling and technology*. John Wiley & Sons, 2014.

E. Baranger. *Modeling Mechanical Behavior of Ceramic Matrix Composites*. 12 2017. ISBN 9780128035818. doi: 10.1016/B978-0-12-803581-8.09993-8.

T. Brepols, S. Wulfinghoff, and S. Reese. Gradient-extended two-surface damage-plasticity: micromorphic formulation and numerical aspects. *International Journal of Plasticity*, 97:64–106, 2017.

T. Brepols, S. Wulfinghoff, and S. Reese. A micromorphic damage-plasticity model to counteract mesh dependence in finite element simulations involving material softening. In *Multiscale Modeling of Heterogeneous Structures*, pages 235–255. Springer, 2018.

J.-L. Chaboche and J.-F. Maire. A new micromechanics based cdm model and its application to cmc's. *Aerospace Science and Technology*, 6(2):131–145, 2002.

K. K. Chawla. *Ceramic matrix composites*. Springer Science & Business Media, 2013.

C. R. Dandekar and Y. C. Shin. Molecular dynamics based cohesive zone law for describing al–sic interface mechanics. *Composites Part A: Applied Science and Manufacturing*, 42(4):355–363, 2011.

A.G. Evans and F.W. Zok. The physics and mechanics of fibre-reinforced brittle matrix composites. *Journal of Materials science*, 29(15):3857–3896, 1994.

M. Fagerström and R. Larsson. A thermo-mechanical cohesive zone formulation for ductile fracture. *Journal of the Mechanics and Physics of Solids*, 56(10):3037–3058, 2008.

S. Forest. Micromorphic approach for gradient elasticity, viscoplasticity, and damage. *Journal of Engineering Mechanics*, 135 (3):117–131, 2009.

Philippe H Geubelle and Jeffrey S Baylor. Impact-induced delamination of composites: a 2d simulation. *Composites Part B: Engineering*, 29(5):589–602, 1998.

S. Guo and Y. Kagawa. Temperature dependence of tensile strength for a woven boron-nitride-coated hi-nicalon sic fiber-reinforced silicon-carbide-matrix composite. *Journal of the American Ceramic Society*, 84(9):2079–2085, 2001.

A. Hattiangadi and T. Siegmund. A thermomechanical cohesive zone model for bridged delamination cracks. *Journal of the Mechanics and Physics of Solids*, 52(3):533–566, 2004.

T. Hinoki, E. Lara-Curzio, and L. L. Snead. Mechanical properties of high purity sic fiber-reinforced cvi-sic matrix composites. *Fusion science and technology*, 44(1):211–218, 2003.

D. Höwer, B. A. Lerch, B. A. Bednarcyk, E. J. Pineda, S. Reese, and J.-W. Simon. Cohesive zone modeling for mode i facesheet to core delamination of sandwich panels accounting for fiber bridging. *Composite Structures*, 183:568–581, 2018.

W. Krenkel. *Ceramic matrix composites: fiber reinforced ceramics and their applications*. John Wiley & Sons, 2008.

R. S. Kumar. Analysis of coupled ply damage and delamination failure processes in ceramic matrix composites. *Acta materialia*, 61(10):3535–3548, 2013.

R. S. Kumar. Crack-growth resistance behavior of mode-i delamination in ceramic matrix composites. *Acta Materialia*, 131: 511–522, 2017.

R. S. Kumar and G. S. Welsh. Delamination failure in ceramic matrix composites: Numerical predictions and experiments. *Acta Materialia*, 60(6-7):2886–2900, 2012.

R. S. Kumar, M. Mordasky, and G. Ojard. Delamination fracture in ceramic matrix composites: From coupons to components. In *ASME Turbo Expo 2018: Turbomachinery Technical Conference and Exposition*, pages V006T02A003–V006T02A003. American Society of Mechanical Engineers, 2018.

L. Marcin, J.-F. Maire, N. Carrère, and E. Martin. Development of a macroscopic damage model for woven ceramic matrix composites. *International Journal of Damage Mechanics*, 20(6):939–957, 2011.

S. K. Mital, B. A. Bednarcyk, S. M. Arnold, and J. Lang. Modeling of melt-infiltrated sic/sic composite properties. 2009.

G. N. Morscher. Tensile creep and rupture of 2d-woven sic/sic composites for high temperature applications. *Journal of the European Ceramic Society*, 30(11):2209–2221, 2010.

Michael Ortiz and Anna Pandolfi. Finite-deformation irreversible cohesive elements for three-dimensional crack-propagation analysis. *International journal for numerical methods in engineering*, 44(9):1267–1282, 1999.

I. Özdemir, W.A.M. Brekelmans, and M.G.D. Geers. A thermo-mechanical cohesive zone model. *Computational Mechanics*, 46 (5):735–745, 2010.

M. Paggi and A. Sapora. Numerical modelling of microcracking in pv modules induced by thermo-mechanical loads. *Energy Procedia*, 38:506–515, 2013.

F. Rebillat, J. Lamon, and A. Guette. The concept of a strong interface applied to sic/sic composites with a bn interphase. *Acta materialia*, 48(18-19):4609–4618, 2000a.

F. Rebillat, J. Lamon, and A. Guette. Importance of fiber/matrix bonding in sic/bn/sic on mechanical and interfacial properties. In *Proceedings of the 12th International Conference on Composite Materials (ICCM12), Paris*, pages 4–9, 2000b.

S. Rezaei, S. Wulfinghoff, and S. Reese. Prediction of fracture and damage in micro/nano coating systems using cohesive zone elements. *International Journal of Solids and Structures*, 121:62–74, 2017.

S. Rezaei, D. Jaworek, J. R. Mianroodi, S. Wulfinghoff, and S. Reese. Atomistically motivated interface model to account for coupled plasticity and damage at grain boundaries. *Journal of the Mechanics and Physics of Solids*, 124:325–349, 2019.

M. Samimi, J.A.W. Van Dommelen, and M.G.D. Geers. An enriched cohesive zone model for delamination in brittle interfaces. *International Journal for Numerical Methods in Engineering*, 80(5):609–630, 2009.

M. Samimi, J.A.W. Van Dommelen, and M.G.D. Geers. A three-dimensional self-adaptive cohesive zone model for interfacial delamination. *Computer Methods in Applied Mechanics and Engineering*, 200(49-52):3540–3553, 2011.

A. Sapora and M. Paggi. A coupled cohesive zone model for transient analysis of thermoelastic interface debonding. *Computational Mechanics*, 53(4):845–857, 2014.

R. W. Trice and J. W. Halloran. Influence of microstructure and temperature on the interfacial fracture energy of silicon nitride/boron nitride fibrous monolithic ceramics. *Journal of the American Ceramic Society*, 82(9):2502–2508, 1999.

T. Wu and P. Wriggers. Multiscale diffusion–thermal–mechanical cohesive zone model for concrete. *Computational Mechanics*, 55(5):999–1016, 2015.